

Adhesion Kinetics of Viable *Cryptosporidium parvum* Oocysts to Quartz Surfaces

ZACHARY A. KUZNAR AND
MENACHEM ELIMELECH*

Department of Chemical Engineering, Environmental
Engineering Program, P.O. Box 208286, Yale University,
New Haven, Connecticut 06520-8286

The transport and deposition (adhesion) kinetics of viable *Cryptosporidium parvum* oocysts onto ultrapure quartz surfaces in a radial stagnation point flow system were investigated. Utilizing an optical microscope and an image-capturing device enabled real time observation of oocyst deposition behavior onto the quartz surface in solutions containing either monovalent (KCl) or divalent (CaCl₂) salts. Results showed a significantly lower oocyst deposition rate in the presence of a monovalent salt compared to a divalent salt. With a monovalent salt, oocyst deposition rates and corresponding attachment efficiencies were relatively low, even at high KCl concentrations where Derjaguin–Landau–Verwey–Overbeek (DLVO) theory predicts the absence of an electrostatic energy barrier. On the other hand, in the presence of a divalent salt, oocyst deposition rates increased continuously as the salt concentration was increased over the entire range of ionic strengths investigated. The unusually low deposition rate in a monovalent salt solution is attributed to “electrosteric” repulsion between the *Cryptosporidium* oocyst and the quartz surface, most likely due to proteins on the oocyst surface that extend into the solution. It is further proposed that specific binding of calcium ions to the oocyst surface functional groups results in charge neutralization and conformational changes of surface proteins that significantly reduce electrosteric repulsion.

Introduction

Cryptosporidium is a protozoan parasite which is able to infect the intestinal tract of its host, causing the disease cryptosporidiosis. It was first described in 1907 in the gastric mucosa of a laboratory mouse (1), but it was not until 1976 that the first human cases were reported, with the individuals suffering from severe diarrhea (2). *Cryptosporidium parvum* has been identified as the only species known to infect humans, and with the onset of the AIDS epidemic in the early 1980s, cryptosporidiosis became known as a life-threatening disease to immunocompromised individuals (3). Waterborne transfer, due to contamination of drinking water supplies from dairy cattle and treated wastewater effluent, is the most common form of indirect transmission of the organism (4).

Cryptosporidium is ubiquitous in aquatic environments, with surveys conducted in several regions of the United States reporting the presence of *Cryptosporidium* in 25 out of 55 surface water samples, and 12 out of 49 wastewater samples

(5). The organism exists as an oocyst in the aquatic environment with a diameter ranging from 4 to 6 μm . The hardy oocyst has been found to be resistant to a number of environmental stresses, including chlorination during drinking water treatment (6). Therefore, deep-bed (granular) filtration or membrane processes are the primary barriers for *Cryptosporidium* oocyst passage in water treatment plants. In addition, natural filtration in alluvial valley aquifers—a process known as bank filtration—is emerging as a viable method of pretreating surface waters for the removal of microbial pathogens such as *Cryptosporidium* oocysts (7).

Due to the threat that *Cryptosporidium* poses to drinking water supplies, numerous studies have investigated the physical and chemical properties of *Cryptosporidium* oocysts in aquatic systems. Results from electrokinetic (ζ) potential characterization report the oocysts to be negatively charged at ambient pH, with the oocyst isoelectric point between 2 and 3 (8–10). In addition, ζ potentials in the range of –19 to –42 mV have been determined at near-neutral pH and moderate ionic strengths (8, 9, 11, 12). Using atomic force microscopy (AFM), Considine et al. (13) reported a substantial repulsive force between a soda-lime glass and viable *Cryptosporidium* oocysts in the presence of both monovalent (potassium chloride) and divalent (calcium nitrate) electrolytes. The magnitude and decay lengths of the measured interaction forces, particularly with KCl, were substantially greater than what would be expected on the basis of classical DLVO interaction. The authors attributed this observation to steric repulsive forces originating from a hairy layer of surface proteins extending into the solution.

Compared to *Cryptosporidium* oocyst characterization, studies on the mechanisms governing the adhesion of oocysts to solid surfaces in aquatic systems are relatively scarce. Hsu et al. (14) studied the influence of ionic strength and pH on the filtration of *Cryptosporidium* oocysts in columns packed with glass and polystyrene beads. Their results showed increased removal of viable oocysts at higher ionic strengths, while lower removal rates were observed with an increase in solution pH. Such filtration behavior is expected on the basis of reduction of electrostatic repulsion between the oocyst and filter collectors.

Despite the efforts discussed above, the mechanisms governing the adhesion of *Cryptosporidium* oocysts to solid surfaces are still poorly understood. In this study, we delineate the mechanisms governing the adhesion of viable *Cryptosporidium* oocysts to solid surfaces under well-controlled chemical and hydrodynamic conditions. A radial stagnation point flow cell, with a well-defined flow field, was used to visualize individual *Cryptosporidium* oocysts as they deposit onto a uniformly charged, flat quartz surface. Utilizing an optical microscope and an image-capturing device, the deposition kinetics of the viable oocysts onto the ultrapure quartz surface were determined in solutions containing either monovalent (KCl) or divalent (CaCl₂) salts. Results suggest that electrosteric repulsion, most likely due to oocyst surface-bound proteins, plays an important role in oocyst adhesion.

Materials and Methods

***Cryptosporidium* Oocyst Source and Preparation.** Viable *Cryptosporidium* oocysts were purchased from the University of Arizona Sterling Parasitology Laboratory (SPL). The oocysts were shed from a calf infected with the Iowa Isolate from Dr. Harley Moon at the National Animal Disease Center in Ames, IA. The oocysts were purified (at SPL) using discontinuous sucrose and cesium chloride centrifugation gradients (15). Oocysts were stored (at 4 °C) in an antibiotic solution

* Corresponding author phone: (203)432-2789; fax: (203)432-2881; e-mail: menachem.elimelech@yale.edu.

containing 0.01% Tween 20, 100 U of penicillin, and 100 μg of gentamicin/mL. Before the experiments were conducted, the oocysts were spun down twice at 12 000 rpm for 1 min, and the supernatant was removed and replaced with 1 mL of deionized water (Barnstead). Purified oocysts were diluted to the desired concentration and suspended in the solution chemistry of interest prior to transport and adhesion experiments. Two separate oocyst batches, denoted 30505-11 and 31103-07, were utilized in the deposition experiments; the batches were shed from different calves on different dates.

Fluorescent microscopy was used to determine the number concentration of *Cryptosporidium* oocysts before the experiments in the radial stagnation point flow system (to be described later). In this procedure, 1 mL of the *Cryptosporidium* oocyst solution was filtered through a 25 mm, 0.22 μm polycarbonate membrane, using a Millipore sampling manifold attached to a dry vacuum pump. After the water was filtered off, the oocysts were stained with a Merifluor-CG detection reagent and counterstain (Meridian Scientific, Cincinnati, OH), and were allowed to sit for 30 min in the dark. After the 30 min, the remaining stain was removed by applying a vacuum for 1 min. Next, a mounting medium (Meridian Scientific) and a 25 mm cover slide (Fisher Scientific, Pittsburgh, PA) were applied to the membrane and placed under an Olympus BX41 fluorescence microscope. To fluoresce the oocysts, the microscope was set to the FITC emission wavelength (excitation at 490 nm, emission at 525 nm), and at least 20 fields at 100 \times were counted. A multiplication factor was used to determine the number of oocysts per milliliter in the sample solution.

Solution Chemistries. Oocyst adhesion (deposition) and electrokinetic characterization experiments were conducted with monovalent (KCl) and divalent (CaCl_2) salts. Experiments were carried out over a range of ionic strengths. For the monovalent salt (KCl), the ionic strength ranged from 1 to 316 mM, while, for the divalent salt (CaCl_2), the ionic strength ranged from 0.1 to 100 mM, corresponding to molar CaCl_2 concentrations from 0.03 to 33.3 mM, respectively. All solutions were unbuffered, resulting in a pH between 5.5 and 5.7.

***Cryptosporidium* Oocyst Characterization.** The electrophoretic mobilities of the *Cryptosporidium* oocysts were determined immediately before a deposition experiment under solution chemistries similar to those used in the corresponding deposition runs. The electrophoretic mobility measurements were performed at 25 $^{\circ}\text{C}$ (± 1 $^{\circ}\text{C}$) using a ZetaPALS analyzer (Brookhaven Instruments Corp., Holtsville, NY). Electrophoretic mobilities were converted to ζ potentials using the Smoluchowski equation. This equation is adequate because of the relatively large size of the oocysts and the ionic strengths used (16). To determine the oocyst average size, images of the oocysts (10^6 oocysts/mL) were taken with an inverted microscope (Axiovert 200m, Zeiss, Thornwood, NY) operating in phase contrast mode. An image-processing program (ImageJ, NIH) was used for analysis of the images and determining the average major and minor axes of the oocysts. The resulting equivalent spherical diameter of the *Cryptosporidium* oocyst was calculated to be 3.7 μm .

Radial Stagnation Point Flow System. A radial stagnation point flow system was utilized for the oocyst deposition (adhesion) experiments. The oocyst suspension was pumped by a syringe pump (model 230, KD Scientific) into a custom-made glass cell through a 2 mm inner diameter capillary tube. Upon emerging from the capillary, the suspension impinges against the transparent quartz cover glass located 2 mm from the capillary opening and flows radially over the cover glass. The oocyst suspension was continuously removed from the cell via a waste stream. Oocyst deposition onto the quartz surface was observed in real time from above by an

optical microscope (Axioplan 2, Zeiss, Thornwood, NY). The microscope images were recorded by a CCD camera (CCD-300-IFG, Dage MTI, Michigan City, IN) and analyzed with image analysis software (KS400, Zeiss). Utilizing the CCD camera, images of oocyst deposition in a 106 $\mu\text{m} \times 80$ μm area at the stagnation point region were captured every minute. The images were analyzed to determine the deposition flux (number of oocysts per area per time), which was used to calculate the oocyst transfer rate in the radial stagnation point flow system.

Quartz Surface Preparation and Characterization. The high-purity (99.9% SiO_2) quartz cover slides (25 mm in diameter and 0.1 mm thick) were obtained from Electron Microscopy Sciences (Ft. Washington, PA). Cover slides were cleaned by soaking in 2% Extran MA02 solution (EM Science, Gibbstown, NJ), followed by rinsing with ethanol (Pharmco Products, Inc., Brookfield, CT) and deionized water (Barnstead). Next, the quartz cover slides were sonicated for 15 min in 2% RBS 35 detergent solution (Pierce, Rockford, IL) and rinsed again with ethanol and deionized (DI) water. The cover slides were then soaked in NOCHROMIX solution (Godax Laboratories, Inc., Takoma Park, MD) for 24 h and thoroughly rinsed with DI water. At this time, the quartz slides were mounted onto the glass flow cell utilized in the radial stagnation point flow system described above.

To create electrostatic conditions favorable for deposition (i.e., positively charged surfaces), the quartz slides were chemically modified using a 0.2% (v/v) mixture of (aminoethylaminomethyl)phenethyltrimethoxysilane (Gelest, Inc., Tullytown, PA) in ethanol. After the aminosilane solution was spread onto the quartz surface, the slide was cured at 130 $^{\circ}\text{C}$ for 90 min, followed by a deionized water rinse. Details on the chemical modification of quartz surfaces with aminosilane are given in our recent publications (17, 18).

The electrokinetic properties of the quartz cover slides were determined by a streaming potential analyzer (EKA, Brookhaven Instruments Corp.) with an asymmetric clamping cell (17). Measurements were obtained in KCl and CaCl_2 over the range of ionic strengths used in the deposition experiments. The instrument was first rinsed with 1 L of deionized water followed by 0.5 L of the electrolyte solution used in the measurement. Prior to the streaming potential measurements being taken, the quartz slide was equilibrated with the corresponding fresh electrolyte solution for 10 min. The ζ potential was calculated from the measured streaming potential as described elsewhere (17).

Adhesion Experiments in the Radial Stagnation Point Flow System. The oocyst deposition rate onto the quartz surface was determined in the presence of monovalent (KCl) or divalent (CaCl_2) salts. Experiments were conducted over the range of ionic strengths discussed previously, with a target oocyst concentration of 2.5×10^6 oocysts/mL. All deposition experiments were repeated at least twice. For each experiment, the influent oocyst concentration was verified by directly visualizing and counting the oocysts using the fluorescence microscopy technique described above. The oocyst suspension was collected during each run in the RSPF system, and the solution ionic strength was raised by adding the necessary amount of a KCl or CaCl_2 solution to achieve the desired ionic strength for the next deposition experiment. Deposition experiments were performed at a flow rate of 9 mL/min corresponding to a capillary Reynolds number of 47.8 and a particle Peclet number of 72.3. For all experiments, the pH was unadjusted (5.5–5.7) and the temperature was fixed at 25 $^{\circ}\text{C}$ (± 1 $^{\circ}\text{C}$).

Determination of Oocyst Deposition Rate and Attachment Efficiency. *Cryptosporidium* oocyst deposition onto

the quartz surface in the radial stagnation point flow system is presented as a transfer rate coefficient, k_D :

$$k_D = \frac{J}{C_0} \quad (1)$$

where J is the oocyst deposition flux and C_0 is the bulk number concentration of *Cryptosporidium* oocysts in solution. The oocyst deposition flux was determined by normalizing the initial slope of the number of deposited oocysts versus time curve by the microscope viewing area ($106 \mu\text{m} \times 80 \mu\text{m}$). The deposition kinetics of *Cryptosporidium* oocysts were also presented in terms of the attachment efficiency, α . The latter was calculated by normalizing the actual oocyst transfer rate coefficient at each ionic strength by the transfer rate coefficient under favorable (nonrepulsive) electrostatic conditions, $k_{D,\text{fav}}$:

$$\alpha = \frac{k_D}{k_{D,\text{fav}}} \quad (2)$$

Favorable electrostatic conditions were achieved in two ways. In the first method, the quartz surface was chemically modified with aminosilane by the procedure outlined earlier to create a net positive charge on the surface. Two runs were performed in the RSPF system with the chemically modified cover slip at 30 mM KCl and ambient pH (5.5–5.7), resulting in an average favorable transfer rate coefficient ($k_{D,\text{fav}}$) of 1.08×10^{-6} m/s. Favorable electrostatic conditions were also achieved by lowering the solution pH to 2.5, rendering oocyst and quartz surface ζ potentials of near zero. Performing two deposition runs with the quartz cover slip at pH 2.5 and at an ionic strength of 30 mM KCl resulted in an average oocyst transfer rate of 1.10×10^{-6} m/s. The nearly identical values obtained with both methods resulted in an average $k_{D,\text{fav}}$ of 1.09×10^{-6} m/s.

Results and Discussion

Electrokinetic Characterization of *Cryptosporidium* Oocysts. The ζ potentials of the *Cryptosporidium* oocysts and quartz surface in the presence of monovalent (KCl) and divalent (CaCl_2) salts are presented in Figure 1. ζ potentials of all surfaces are negatively charged at the pH of the experiments (5.5–5.7), and become less negative with increases in the ionic strength in the presence of both the monovalent and divalent electrolyte solutions. The decrease in ζ potential with increasing KCl concentration is attributed to double-layer compression, while, with a divalent (CaCl_2) salt, specific binding of Ca^{2+} to surface functional groups and subsequent charge neutralization also take place as evidenced by the much greater reduction in the absolute value of the ζ potential. Thomas et al. (19) found similar results with divalent salts, reporting a near-neutral ζ potential (–2 mV) of *Cryptosporidium* oocysts in 0.01 M CaCl_2 at pH 7.0. The ζ potentials shown in Figure 1 will be used later to calculate the DLVO interaction energies between the oocysts and the quartz surface.

An interesting observation in the ζ potential versus KCl curves is the significant difference between the ζ potential behaviors of the two oocyst batches. For instance, at a KCl concentration of 1 mM, the ζ potentials of the different batches are –17.2 and –30.6 mV. It should be noted that these two oocyst batches were shed from different calves, but underwent identical purification techniques. The observed variation in ζ potential is consistent with previously reported literature values: $-37 \text{ mV} < \zeta < -42 \text{ mV}$ at neutral pH for viable oocysts (11), $-19 \text{ mV} < \zeta < -36 \text{ mV}$ in 1 mM NaCl at pH 6 for viable oocysts (8), $\zeta = -25 \pm 2.8 \text{ mV}$ in DI water at pH 6 for viable oocysts (9), and $\zeta \approx -22 \text{ mV}$ in DI water at pH 6 for heat-inactivated oocysts (20).

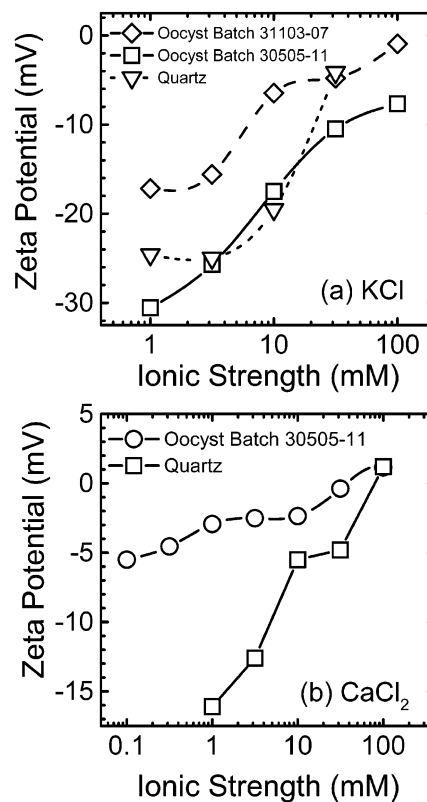


FIGURE 1. (a) ζ potentials of viable *Cryptosporidium* oocysts (batches 31103-07 and 30505-11) and quartz cover slip as a function of ionic strength (KCl) at pH 5.5–5.7. (b) ζ potentials of viable *Cryptosporidium* oocysts (batch 30505-11) and quartz cover slip as a function of ionic strength (CaCl_2) at pH 5.5–5.7.

Current knowledge of the chemical composition of the oocyst wall is limited. Previous studies (8, 9, 20) have shown that the oocyst surface is negatively charged at pH values greater than 3.5. Although the nature of the surface groups has not been identified, it has been determined that the surface of the *Cryptosporidium* oocyst wall contains cysteine, proline, and histidine (21). On the basis of a fitted $\text{p}K_a$ value of 2.5, Karaman et al. (8) suggested the presence of carboxylate and/or phosphate groups, which would lead to the overall negative charge at the pH range investigated (5.5–5.7). The carboxylate groups could be associated with the cysteine-rich proteins and glycoproteins on the oocyst surface (8).

Deposition Rate of *Cryptosporidium* Oocysts in the Presence of a Monovalent Electrolyte. The oocyst transfer rate coefficient (k_D) and the corresponding attachment efficiency (α) as a function of KCl concentration are presented in Figure 2a. As can be seen, the transfer rate and attachment efficiency of the viable *Cryptosporidium* oocysts onto the quartz cover slip are negligible over the entire range of ionic strengths investigated. The attachment efficiency remains zero up to an ionic strength of 177 mM, and increases to a value of 0.03 at an ionic strength of 316 mM. It should be emphasized that the zero attachment efficiency means that, under the employed experimental conditions, no measurable oocyst deposition could be observed over the 20 min deposition run. To explain the observed deposition behavior, particularly the negligible deposition rate at such high ionic strengths, we resort to DLVO interaction energy calculations as described below.

The total interaction energy was calculated as the sum of electrostatic and van der Waals interactions. The repulsive

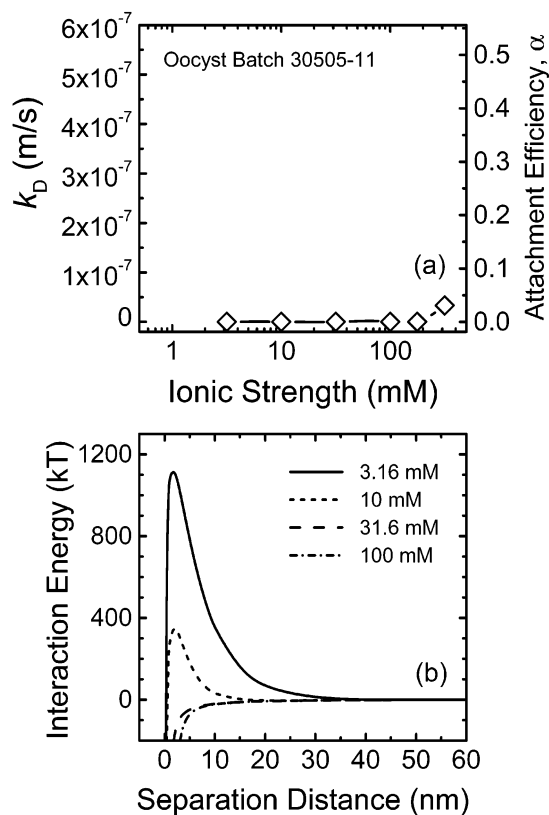


FIGURE 2. (a) *Cryptosporidium* oocyst deposition kinetics (batch 30505-11) onto the quartz surface as a function of ionic strength (KCl). The deposition kinetics are expressed as oocyst transfer rate, k_b , and attachment efficiency, α . Experimental conditions were as follows: capillary flow rate in the RSPF 9.0 mL/min (average velocity 4.77 cm/s), pH 5.5–5.7, and temperature 25 °C (± 1 °C). (b) Calculated DLVO interaction energy profiles between a *Cryptosporidium* oocyst (batch 30505-11) and a quartz surface as a function of separation distance for various ionic strengths (KCl). Interaction energies were calculated from the experimentally determined ζ potentials (Figure 1) assuming a value of the Hamaker constant of 6.5×10^{-21} J and an oocyst diameter of 3.7 μm .

electrostatic double-layer interaction energy was calculated using the Hogg et al. (22) expression

$$\phi_{\text{EDL}} = \pi\epsilon_0\epsilon_r a_p \left\{ 2\psi_p\psi_c \ln \left[\frac{1 + \exp(-\kappa h)}{1 - \exp(-\kappa h)} \right] + (\psi_p^2 + \psi_c^2) \ln[1 - \exp(-2\kappa h)] \right\} \quad (3)$$

where ϵ_0 is the dielectric permittivity in a vacuum, ϵ_r is the relative dielectric permittivity of water, a_p is the oocyst radius, κ is the inverse Debye length, h is the separation distance between the *Cryptosporidium* oocyst and the quartz surface, and ψ_p and ψ_c are the surface (ζ) potentials of the *Cryptosporidium* oocyst and quartz surface, respectively. The retarded van der Waals attractive interaction energy was calculated by using (23)

$$\phi_{\text{VDW}} = -\frac{Aa_p}{6h} \left[1 + \frac{14h}{\lambda} \right]^{-1} \quad (4)$$

where λ is the characteristic wavelength of the dielectric (assumed to be 100 nm) and A is the Hamaker constant of the interacting medium. In the absence of literature values for the Hamaker constant of the oocyst–water–quartz medium, we have chosen a value of 6.5×10^{-21} J, similar to that reported for bacterial cells interacting with quartz in an aqueous medium (24–26).

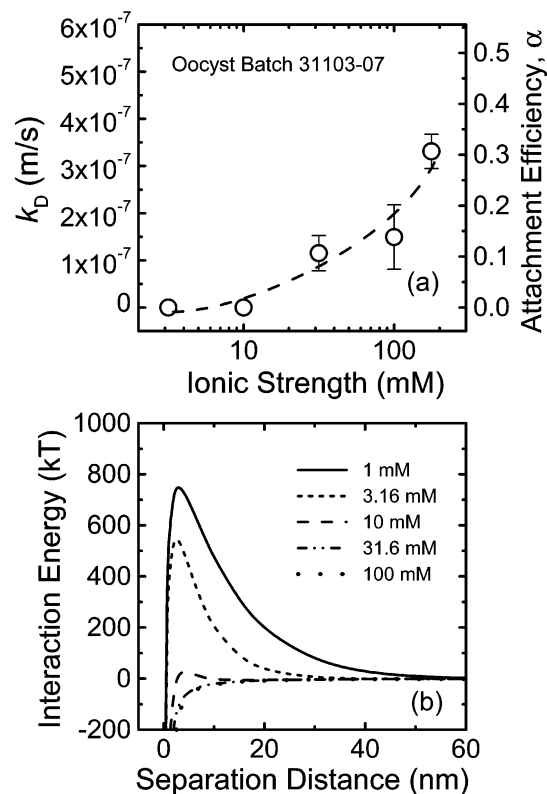


FIGURE 3. (a) *Cryptosporidium* oocyst deposition kinetics (batch 31103-07) onto the quartz surface as a function of ionic strength (KCl). The deposition kinetics are expressed as oocyst transfer rate, k_b , and attachment efficiency, α . Experimental conditions were as follows: capillary flow rate in the RSPF 9.0 mL/min (average velocity 4.77 cm/s), pH 5.5–5.7, and temperature 25 °C (± 1 °C). (b) Calculated DLVO interaction energy profiles between a *Cryptosporidium* oocyst (batch 31103-07) and a quartz surface as a function of separation distance for various ionic strengths (KCl). Interaction energies were calculated from the experimentally determined ζ potentials (Figure 1) assuming a value of the Hamaker constant of 6.5×10^{-21} J and an oocyst diameter of 3.7 μm .

The calculated DLVO interaction energy profiles (Figure 2b) demonstrate that sizable repulsive energy barriers exist up to an ionic strength of 10 mM, ranging from over 1100 kT at 3.16 mM to 367 kT at 10 mM. Such high energy barriers inhibit the deposition of *Cryptosporidium* oocysts onto the quartz surface. However, at ionic strengths greater than 10 mM, electrostatic energy barriers cease to exist. Interestingly, despite the absence of an energy barrier, no measurable oocyst deposition was observed up to an ionic strength of 177 mM (or $10^{-0.75}$ M). Even at a very high ionic strength of 316 mM ($10^{-0.5}$ M), the oocyst deposition rate was very low, resulting in $\alpha = 0.03$.

The deposition kinetics for a second batch of oocysts in the presence of KCl and the corresponding DLVO interaction energy profiles are presented in Figure 3. As demonstrated earlier (Figure 1), the oocysts in this batch have less negative ζ potentials compared to those in the batch used in the experiments presented earlier in Figure 2. The deposition rate of the oocyst (Figure 3a) is higher than that observed for the previous batch, but the attachment efficiency is still much lower than unity over the entire range of ionic strengths studied. It can further be seen from the DLVO interaction energy profiles that, as with the previous batch, sizable energy barriers exist up to an ionic strength of 10 mM, ranging from over 750 kT at 1 mM to 27 kT at 10 mM. As observed in Figure 3a, such high energy barriers inhibit deposition of oocysts onto the quartz surface. At ionic strengths greater than 10

mM, electrostatic energy barriers are absent. However, the oocyst attachment efficiency is still far from unity even though favorable electrostatic conditions for oocyst deposition exist.

From the preceding experimental data, it can be seen that classic DLVO theory drastically overpredicts the deposition rate of the viable oocysts onto the quartz surface in the presence of a monovalent salt. This observation suggests the presence of an additional non-DLVO repulsive force that prevents oocyst attachment. As discussed in more detail later in this paper, we propose the presence of a steric repulsive force, originating from the protein layer on the oocyst surface, which significantly reduces the oocyst deposition rate.

Is Deposition in the Secondary Minimum Relevant for the RSPF System? Due to the large size of the *Cryptosporidium* oocysts, a deep secondary minimum energy well exists for the investigated ionic strengths where electrostatic energy barriers prevent irreversible deposition onto the quartz surface. However, in the stagnation point flow system, *Cryptosporidium* oocysts that are entrained in the secondary minimum experience a hydrodynamic force in the radial direction. This radial hydrodynamic force will sweep the oocysts out of the field of view of the stagnation point ($106 \mu\text{m} \times 80 \mu\text{m}$), and therefore, only particles that are deposited irreversibly in the primary minimum will be enumerated. In this way, studying particle deposition in the radial stagnation point flow system differs from column experiments where spherical collector grains are used. When using spherical collector grains, oocysts that deposit in the secondary energy minimum translate along the grain surface and accumulate in either the rear stagnation point of the collector or other regions of stagnant flow on the collector grain created by grain surface irregularities (24, 27). Therefore, deposition in both the primary and secondary minima will occur when column experiments are performed, while only primary minimum deposition takes place when experiments with the radial stagnation point flow system are performed.

The particle velocity in the vicinity of the stagnation point flow region can be calculated from (16, 28, 29)

$$u_r = f_3(H) \frac{\hat{\alpha}_{\text{RSPF}} V_0}{R^2} (h + a_p) r \quad (5)$$

where $\hat{\alpha}_{\text{RSPF}}$ is a flow parameter that is calculated numerically and depends on both the Reynolds number and the geometry of the system, V_0 is the average velocity of the fluid in the capillary, R is the radius of the RSPF capillary, h is the surface-to-surface separation distance between the *Cryptosporidium* oocyst and the quartz surface, a_p is the oocyst radius, r is the distance from the stagnation point in the radial direction, and $f_3(H)$ is a universal function to account for hydrodynamic (viscous) interactions, which depends on the dimensionless separation distance ($H = h/a_p$). Goldman et al. (16, 30) presented an approximate expression for this function at close separation distances ($H \rightarrow 0$) which applies quite well to typical distances of the secondary minimum from the quartz surface:

$$f_3(H) \approx \frac{0.7431}{0.6376 - 0.200 \ln H} \quad (6)$$

Equations 5 and 6 were used to calculate the average radial velocity of *Cryptosporidium* oocysts in the secondary minimum over a $50 \mu\text{m}$ radial distance in the RSPF system. The average velocity over the $50 \mu\text{m}$ distance is considered since the velocity is a function of the radial distance from the stagnation point (eq 5). Table 1 presents the variation of the secondary minimum depth and the distance of the secondary minimum from the quartz surface as a function of ionic strength, as well as the predicted average oocyst velocity in the radial direction of the stagnation point flow region at a

TABLE 1. Variation of the Secondary Minimum Depth and Separation Distance from the Quartz Surface as a Function of Ionic Strength (1:1 Electrolyte) along with the Calculated Oocyst Average Radial Velocity in the Secondary Minimum

| ionic strength (mM) | secondary min depth (kT) | secondary min separation (nm) | avg oocyst velocity ($\mu\text{m/s}$) |
|------------------------------|--------------------------|-------------------------------|---|
| Oocyst Batch 31103-07 | | | |
| 1 | -0.25 | 110 | 44.2 |
| 3.16 | -0.97 | 50 | 38.4 |
| 10 | -4.5 | 20 | 33.2 |
| 31.6 | NB ^a | NB | NB |
| 100 | NB | NB | NB |
| 177 | NB | NB | NB |
| 316 | NB | NB | NB |
| Oocyst Batch 30505-11 | | | |
| 1 | -0.29 | 100 | 44.1 |
| 3.16 | -1.06 | 50 | 38.4 |
| 10 | -6.89 | 15 | 31.8 |
| 31.6 | NB | NB | NB |
| 100 | NB | NB | NB |

^a No calculated barrier to deposition (i.e., no secondary minimum).

separation distance equal to the location of the secondary minimum away from the collector surface. As can be seen from the table, the average velocity over the $50 \mu\text{m}$ distance is greater than $30 \mu\text{m/s}$ for each ionic strength. Therefore, the oocyst will be swept away from the stagnation point flow region in less than 2 s when entrained in the secondary energy minimum. The theoretical times calculated for oocysts to be swept from the stagnation region are on the same order of magnitude as those observed experimentally for the *Cryptosporidium* oocysts via the microscopic system.

***Cryptosporidium* Oocyst Deposition Kinetics in the Presence of a Divalent Electrolyte.** The oocyst transfer rate coefficient (k_p) and attachment efficiency (α) in the presence of a divalent, 2:1 electrolyte (CaCl_2) are presented in Figure 4a. Deposition of oocysts begins at an ionic strength as low as 0.316 mM and rises steadily up to an ionic strength of 100 mM. According to the calculated DLVO interaction energy profiles (Figure 4b), a repulsive energy barrier exists up to 1 mM, ranging from 67 kT at 0.316 mM to 17 kT at 1 mM. Such electrostatic energy barriers should, in principle, prevent deposition of *Cryptosporidium* oocysts onto the quartz surface. However, divalent cations can chemically bind to negatively charged functional groups (via complex formation) and effectively neutralize the surface charge (31, 32); such chemical effects are not accounted for in classical DLVO theory. Hence, the observed oocyst deposition at very low calcium chloride concentrations and the gradual increase in deposition rate with salt concentration are attributed to the binding of Ca^{2+} to protein functional groups on the oocyst surface and substantial reduction in electrostatic repulsion. Binding of Ca^{2+} to protein and the resulting charge neutralization can also result in protein conformational changes and reduction of electrosteric repulsion as discussed later in the paper. Supporting evidence for these mechanisms can be found in the AFM study of Considine et al. (13), where substantial reduction in the magnitude and range of the repulsive force between an oocyst and a glass surface was obtained in the presence of calcium ions.

Comparison of oocyst deposition kinetics with monovalent and divalent salts is presented in Figure 5. It is obvious that, in the presence of a divalent salt, the oocyst transfer rate is much higher than with the corresponding ionic strength of a monovalent salt. It should be noted that the oocysts used in the experiments with KCl which resulted in nonmeasurable deposition (ionic strength lower than 316 mM) are from the same batch as those performed in the

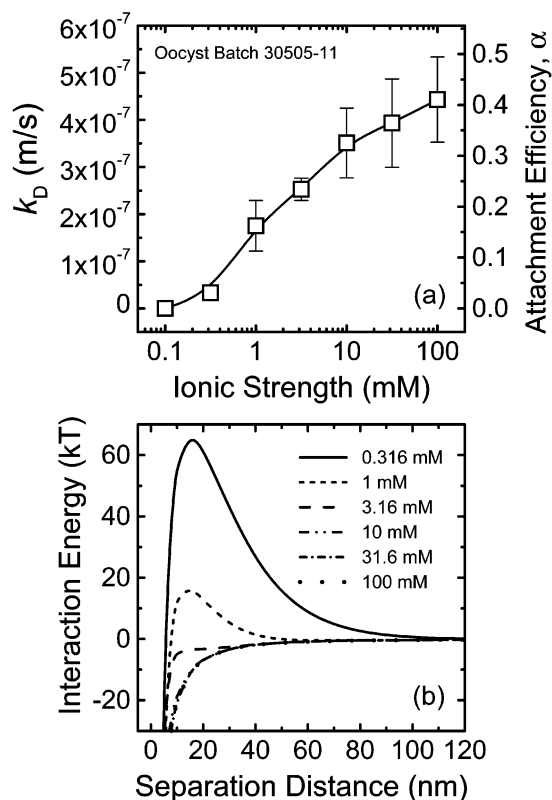


FIGURE 4. (a) *Cryptosporidium* oocyst deposition kinetics (batch 30505-11) onto the quartz surface as a function of the ionic strength of a divalent electrolyte (CaCl_2). The deposition kinetics are expressed as oocyst transfer rate, k_D , and attachment efficiency, α . Experimental conditions were as follows: capillary flow rate in the RSPF 9.0 mL/min (average velocity 4.77 cm/s), pH 5.5–5.7, and temperature 25 °C (± 1 °C). (b) Calculated DLVO interaction energy profiles between a *Cryptosporidium* oocyst (batch 30505-11) and a quartz surface as a function of separation distance for various ionic strengths of a divalent electrolyte (CaCl_2). Interaction energies were calculated from the experimentally determined ζ potentials (Figure 1) assuming a value of the Hamaker constant of 6.5×10^{-21} J and an oocyst diameter of 3.7 μm .

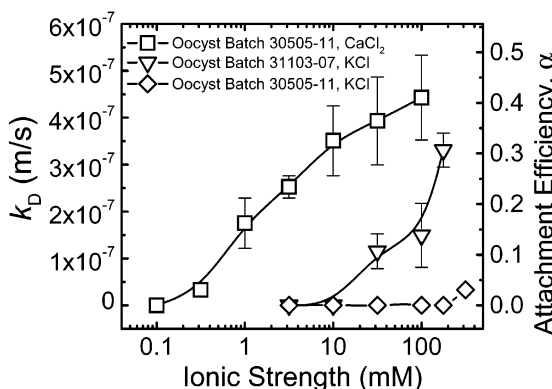


FIGURE 5. Comparison of *Cryptosporidium* oocyst deposition kinetics for monovalent (KCl) and divalent (CaCl_2) electrolytes. Details are given in Figures 2–4.

divalent salt. Oocysts from the same batch come from the same calf, and are collected and purified from the same shed event. This emphasizes the drastic differences in deposition rate with monovalent compared to divalent electrolytes. It further underscores our assertion that DLVO theory drastically overpredicts the deposition rate of *Cryptosporidium* oocysts in the presence of KCl. As discussed below, an electrosteric repulsion between the oocyst surface proteins

and the quartz surface is suggested as the cause for this deviation from classical DLVO theory in the monovalent salt.

Mechanisms Controlling *Cryptosporidium* Oocyst Adhesion. The observed attachment efficiency of *Cryptosporidium* oocysts onto the quartz surface is unusually low in a monovalent salt, even at a high KCl concentration when no electrostatic barrier to deposition exists. However, in the presence of a divalent salt, the attachment efficiency increases with salt concentration over the entire range of ionic strengths investigated. This behavior points to an additional repulsive force that cannot be captured by classic DLVO theory. We propose an electrosteric repulsion between the oocysts and the quartz surfaces.

Electrosteric repulsion is relevant to surfaces containing polyelectrolytes where both electrostatic and steric repulsive forces are present (16, 31, 33, 34). The electrostatic component originates from the presence of charged functional groups on the particle surface and/or the polyelectrolytes. Steric repulsion, on the other hand, is attributed to the compression of surface polymers upon contact with another surface (31). Several studies addressing interactions between particles and surfaces support the presence of electrosteric repulsion (13, 33, 35, 36).

Previous studies involving characterization of *Cryptosporidium* oocysts suggest that the oocyst surface possesses anchored glycoproteins (13, 37). These macromolecules are probably stretched into the solution due to electrostatic repulsion of surface ionizable groups distributed along the polypeptide backbone. We surmise that this brushlike structure of surface proteins imparts steric repulsion which significantly hinders oocyst deposition.

As the ionic strength of the 1:1 electrolyte (KCl) is raised, charge screening of the protein functional groups occurs. Though the transfer rate increases with increasing ionic strength (in the 1:1 electrolyte), the attachment efficiency remains unusually low due to the very strong electrosteric repulsion. With a 2:1 electrolyte (CaCl_2), the transfer rate and corresponding attachment efficiency rise considerably over the range of ionic strengths investigated. This behavior is attributed to binding of the divalent cations to the functional groups along the protein polypeptide (31, 32, 38, 39). We hypothesize that charge neutralization of the surface proteins results in conformational changes and subsequent collapse of the proteins which eliminate steric repulsion. Thus, with divalent cations, the combined effects of protein conformational changes along with reduction in the range of electrostatic interactions yield higher oocyst attachment efficiency.

Acknowledgments

Research was supported by the U.S. Department of Agriculture, Grant 2002-35102-12600.

Literature Cited

- 1) Tyzzer, E. E. A sporozoan found in the peptic glands of the common mouse. *Proc. Soc. Exp. Biol. Med.* **1907**, 5, 12–13.
- 2) Meisel, J. L.; Perera, D. R.; Meligro, C.; Rubin, C. E. Overwhelming watery diarrhea associated with *Cryptosporidium* in an immunosuppressed patient. *Gastroenterology* **1976**, 70, 1156–1160.
- 3) Tzipori, S.; Ward, H. *Cryptosporidiosis*: biology, pathogenesis, and disease. *Microbes Infect.* **2002**, 4, 1047–1058.
- 4) Walker, M. J.; Montemagno, C. D.; Jenkins, M. B. Source water assessment and non-point sources of acutely toxic contaminants: A review of research related to survival and transport of *Cryptosporidium parvum*. *Water Resour. Res.* **1998**, 34, 3383–3392.
- 5) Xiao, L.; Singh, A.; Limor, J.; Graczyk, T. K.; Gradus, S.; Lal, A. Molecular characterization of *Cryptosporidium* oocysts in samples of raw surface water and wastewater. *Appl. Environ. Microbiol.* **2001**, 67, 1097–1101.

- (6) Widmer, G.; Carraway, M.; Tzipori, S. Water-borne *Cryptosporidium*: A perspective from the USA. *Parasitol. Today* **1996**, *12*, 286–290.
- (7) Tufenkji, N.; Ryan, J. N.; Elimelech, M. The promise of bank filtration. *Environ. Sci. Technol.* **2002**, *36*, 422a–428a.
- (8) Karaman, M. E.; Pashley, R. M.; Bustamante, H.; Shanker, S. R. Micro-electrophoresis of *Cryptosporidium parvum* oocysts in aqueous solutions of inorganic and surfactant cations. *Colloids Surf., A* **1999**, *146*, 217–225.
- (9) Drozd, C.; Schwartzbrod, J. Hydrophobic and electrostatic cell surface properties of *Cryptosporidium parvum*. *Appl. Environ. Microbiol.* **1996**, *62*, 1227–1232.
- (10) Lytle, D. A.; Johnson, C. H.; Rice, E. W. A systematic comparison of the electrokinetic properties of environmentally important microorganisms in water. *Colloids Surf., B* **2002**, *24*, 91–101.
- (11) Hsu, B. M.; Huang, C. P. Influence of ionic strength and pH on hydrophobicity and zeta potential of *Giardia* and *Cryptosporidium*. *Colloids Surf., A* **2002**, *201*, 201–206.
- (12) Ongerth, J. E.; Pecoraro, J. P. Electrophoretic mobility of *Cryptosporidium* oocysts and *Giardia* cysts. *J. Environ. Eng.* **1996**, *122*, 228–231.
- (13) Considine, R. F.; Dixon, D. R.; Drummond, C. J. Oocysts of *Cryptosporidium parvum* and model sand surfaces in aqueous solutions: An atomic force microscope (AFM) study. *Water Res.* **2002**, *36*, 3421–3428.
- (14) Hsu, B. M.; Huang, C. P.; Pan, J. R. Filtration behaviors of *Giardia* and *Cryptosporidium*—ionic strength and pH effects. *Water Res.* **2001**, *35*, 3777–3782.
- (15) Brush, C. F.; Walter, M. F.; Anguish, L. J.; Ghiorse, W. C. Influence of pretreatment and experimental conditions on electrophoretic mobility and hydrophobicity of *Cryptosporidium parvum* oocysts. *Appl. Environ. Microbiol.* **1998**, *64*, 4439–4445.
- (16) Elimelech, M.; Gregory, J.; Jia, X.; Williams, R. A. *Particle Deposition and Aggregation—Measurement, Modelling and Simulation*; Butterworth-Heinemann: Woburn, MA, 1995.
- (17) Walker, S. L.; Bhattacharjee, S.; Hoek, E. M. V.; Elimelech, M. A novel asymmetric clamping cell for measuring streaming potential of flat surfaces. *Langmuir* **2002**, *18*, 2193–2198.
- (18) Elimelech, M.; Chen, J. Y.; Kuznar, Z. A. Particle deposition onto solid surfaces with micropatterned charge heterogeneity: The hydrodynamic bump effect. *Langmuir* **2003**, *19*, 6594–6597.
- (19) Thomas, F.; Bard, E.; Rouillier, M. C.; Prelot, B.; Mathieu, L. Filtration-elution of *Cryptosporidium* oocysts assisted by electrostatic interactions. *Colloids Surf., A* **2001**, *195*, 135–142.
- (20) Ongerth, J. E.; Hutton, P. E. Testing of diatomaceous filtration for removal of *Cryptosporidium* oocysts. *J. Am. Water Works Assoc.* **2001**, *93*, 54–63.
- (21) Ranucci, L.; Müller, H. M.; Larosa, G.; Reckmann, I.; Morales, M. A. G.; Spano, F.; Pozio, E.; Crisanti, A. Characterization and immunolocalization of a *Cryptosporidium* protein containing repeated amino-acid motifs. *Infect. Immun.* **1993**, *61*, 2347–2356.
- (22) Hogg, R.; Healy, T. W.; Fuersten, D. W. Mutual coagulation of colloidal dispersions. *Trans. Faraday Soc.* **1966**, *62*, 1638.
- (23) Gregory, J. Approximate expressions for retarded van der Waals interactions. *J. Colloid Interface Sci.* **1981**, *83*, 138–145.
- (24) Redman, J. A.; Walker, S. L.; Elimelech, M. Bacterial adhesion and transport in porous media: Role of the secondary energy minimum. *Environ. Sci. Technol.* **2004**, *38*, 1777–1785.
- (25) Simoni, S. F.; Bosma, T. N. P.; Harms, H.; Zehnder, A. J. B. Bivalent cations increase both the subpopulation of adhering bacteria and their adhesion efficiency in sand columns. *Environ. Sci. Technol.* **2000**, *34*, 1011–1017.
- (26) Truesdail, S. E.; Lukasik, J.; Farrah, S. R.; Shah, D. O.; Dickinson, R. B. Analysis of bacterial deposition on metal (hydr)oxide-coated sand filter media. *J. Colloid Interface Sci.* **1998**, *203*, 369–378.
- (27) Spielman, L. A. Particle capture from low speed laminar flows. *Annu. Rev. Fluid Mech.* **1977**, *9*, 297–319.
- (28) Dabros, T.; van de Ven, T. G. M. Deposition of latex particles on glass surfaces in an impinging jet. *PhysicoChem Hydrodynamics* **1987**, *8*, 171.
- (29) Dabros, T.; van de Ven, T. G. M. A direct method for studying particle deposition onto solid surfaces. *Colloid Polym. Sci.* **1983**, *261*, 694.
- (30) Goldman, A. J.; Cox, R. J.; Brenner, H. Slow viscous motion of a sphere parallel to a plane wall, I. Motion through a quiescent fluid, II. Couette flow. *Chem. Eng. Sci.* **1967**, *22*, 637–651, 653–660.
- (31) Israelachvili, J. *Intermolecular and Surface Forces*, 2nd ed.; Academic Press Inc.: San Diego, CA, 1992.
- (32) Stumm, W.; Morgan, J. J. *Aquatic Chemistry, Chemical Equilibria and Rates in Natural Waters*, 3rd ed.; John Wiley & Sons, Inc.: New York, 1996.
- (33) Pedersen, H. G.; Bergstrom, L. Forces measured between zirconia surfaces in poly(acrylic acid) solutions. *J. Am. Ceram. Soc.* **1999**, *82*, 1137–1145.
- (34) Hunter, R. J. *Foundations of Colloid Science*, 2nd ed.; Oxford University Press: New York, 2001.
- (35) Comesano, T. A.; Logan, B. E. Probing bacterial electrosteric interactions using atomic force microscopy. *Environ. Sci. Technol.* **2000**, *34*, 3354–3362.
- (36) Rijnaarts, H. H. M.; Norde, W.; Lyklema, J.; Zehnder, A. J. B. DLVO and steric contributions to bacterial deposition in media of different ionic strengths. *Colloids Surf., B* **1999**, *14*, 179–195.
- (37) Harris, J. R.; Petry, F. *Cryptosporidium parvum*: structural components of the oocyst wall. *J. Parasitol.* **1999**, *85*, 839–849.
- (38) Andre, I.; Linse, S. Measurement of Ca²⁺ binding constants of proteins and presentation of the CaLigator software. *Anal. Biochem.* **2002**, 195–205.
- (39) Miklavcic, S. J.; Thulin, E.; Joensson, B. Forces between macroscopic surfaces in solutions of calcium binding proteins. *J. Phys. Chem.* **1996**, *100*, 5554–5561.

Received for review April 20, 2004. Revised manuscript received September 7, 2004. Accepted September 13, 2004.

ES0494104